RESEARCH ARTICLE

Figures and figure supplements

Osterix-Cre marks distinct subsets of CD45- and CD45+ stromal populations in extra-skeletal tumors with pro-tumorigenic characteristics

Biancamaria Ricci *et al*

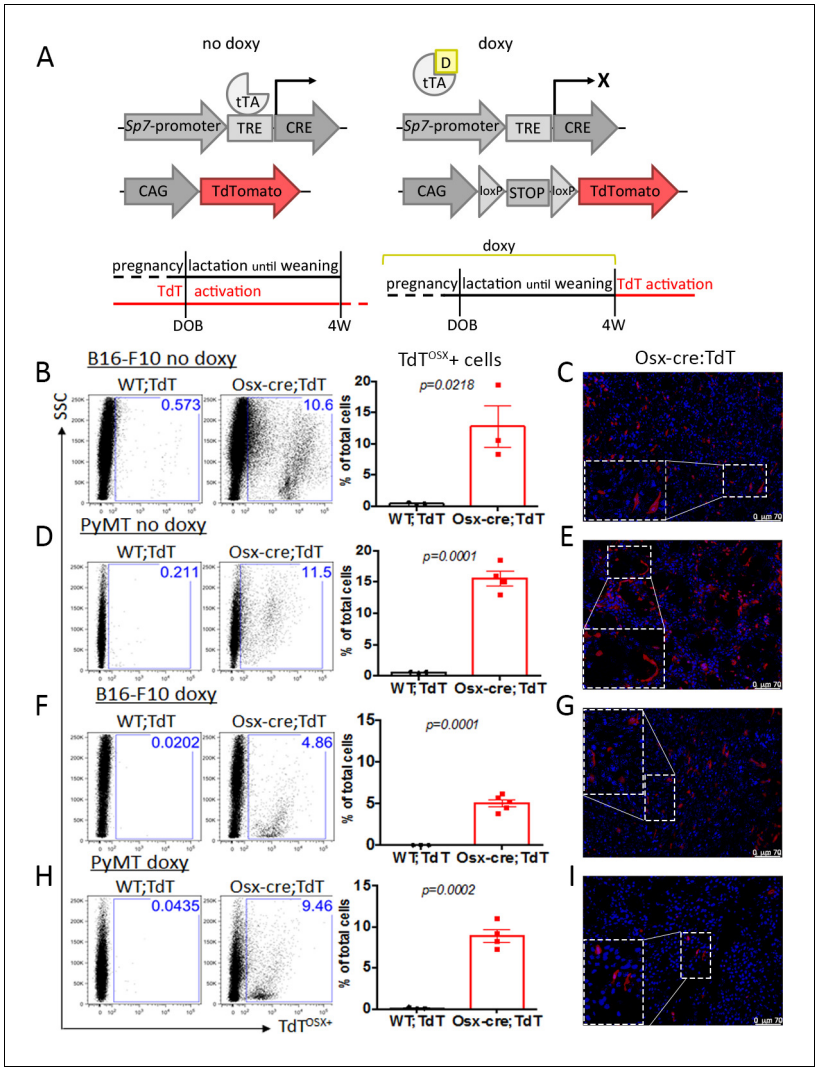

Figure 1. Embryonic and adult-derived Osx+ cells are present in primary tumors at extra-skeletal sites. (**A**) Doxycycline (doxy)-repressible Sp7-cre/loxP mouse model used to activate Ai9/TdTomato expression for lineage tracing experiments. In no doxy-fed mice, TdT is expressed in embryonic-derived osteolineage cells (left), while in mice fed a doxy diet until weaning, TdT is expressed in adult-derived osteolineage cells. (**B–I**) Flow cytometry analysis and fluorescence images of primary tumors showing presence of TdT^{OSX}+ cells in no-doxy fed Osx-cre; TdT mice or WT;TdT controls inoculated with B16-F10 melanoma subcutaneously (**B–C**), or with PyMT breast cancer cells in the mammary fat pad (MFP) (**D–E**), and in doxy-fed mice injected with B16-F10 subcutaneously (**F–G**), or with PyMT in the MFP (**H–I**). Slides for fluorescence images were counterstained with DAPI (blue), magnification 200X. Inserts are further magnified 4.5 folds. Data representative of a single experiment, experiments were repeated between 2 and 5 times. p values represent Student t-test statistical analysis.

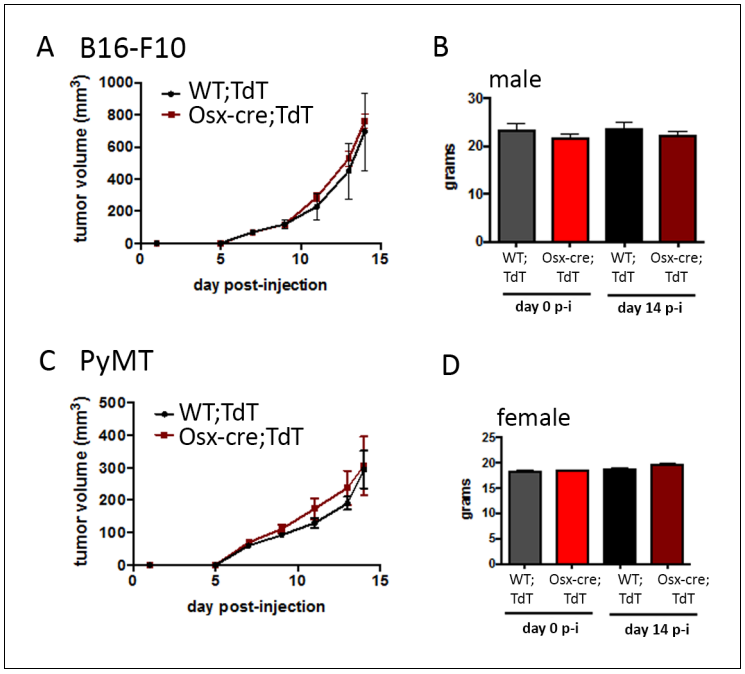

Figure 1—figure supplement 1. No difference in tumor growth and body weight between sex and age matched cre positive (Osx-cre;TdT) and negative (WT;TdT) mice. . (**A**) Tumor growth in Osx-cre;TdT and WT;TdT male mice injected subcutaneously with B16-F10 tumor cells. (**B**) Body weight of the mice showed in (**A**) at the day of tumor injection (day 0) and at the end point (day 14 post-injection). (**C**) Tumor growth in Osx-cre;TdT and WT;TdT female mice injected in the MFP with PyMT tumor cells. (**D**) Body weight of the mice showed in (**C**) on day 0 and day 14 post-injection.

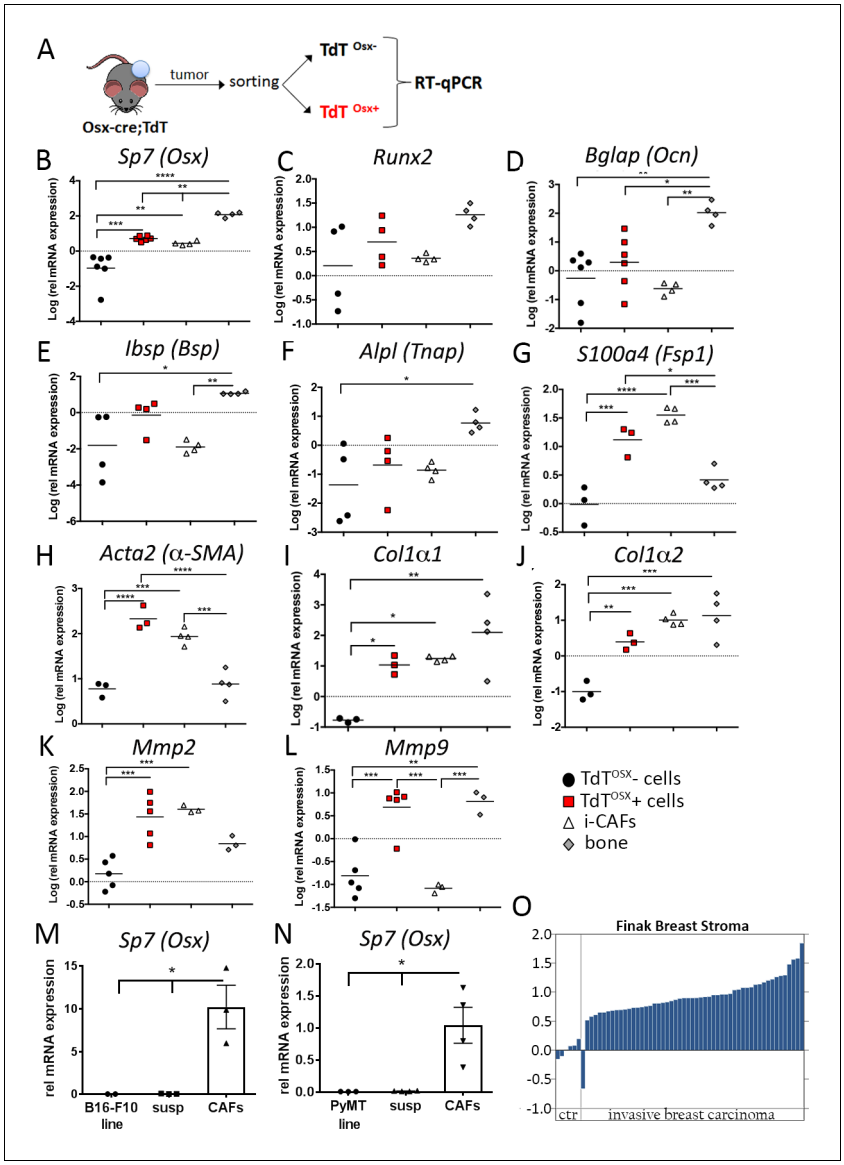

Figure 2. TdT^{OSX}+ cells from primary tumors express mesenchymal markers. (**A**) Experimental design for isolating TdT^{OSX}+ cells from primary tumors isolated from doxy-fed Osx-cre;TdT mice inoculated with B16-F10. TdT^{OSX}- cells comprise all TdT negative cells including the tumor cells. Immortalized CAFs (iCAFs) and crushed long bones were used as reference controls. (**B–L**) Quantitative Real-Time PCR for (**B**) *Sp7(Osterix)*, (**C**) *Runx2*, (**D**) *Bglap (Osteocalcin)*, (**E**) *Ibsp (Bone sialoprotein)*, (**F**) *Alpl (Tnap, Tissue non-specific alkaline phosphatase)*, (**G**) *S100a4 (Fsp1)*, (**H**) *Acta2 (α-SMA)* (**I**) *Collagen1a1* (**J**) *Collagen1a2*, (**K**) *Mmp2 (Metalloproteinase2)* and (**L**) *Mmp9 (Metalloproteinase9)* genes in TdT^{OSX}+, TdT^{OSX}- cells, iCAFs and bone. Each data point includes cells isolated from 3 to 4 mice and from two independent experiments. (**M–N**) Real-Time PCR of *Sp7(Osterix)* in B16-F10 or PyMT cell lines, CAFs isolated from primary B16-F10 or PyMT tumors or from the remaining cells comprising the tumor minus the CAFs (susp) (n = 3–4 mice). (**O**) *Sp7(Osx)* expression based on the Finak Breast Cancer Stroma gene set in the Oncomine cancer microarray database. Significance was determined by one-way ANOVA with Tukey post-hoc test, *p<0.05, **p<0.01, ***p<0.001, ****p<0.0001.

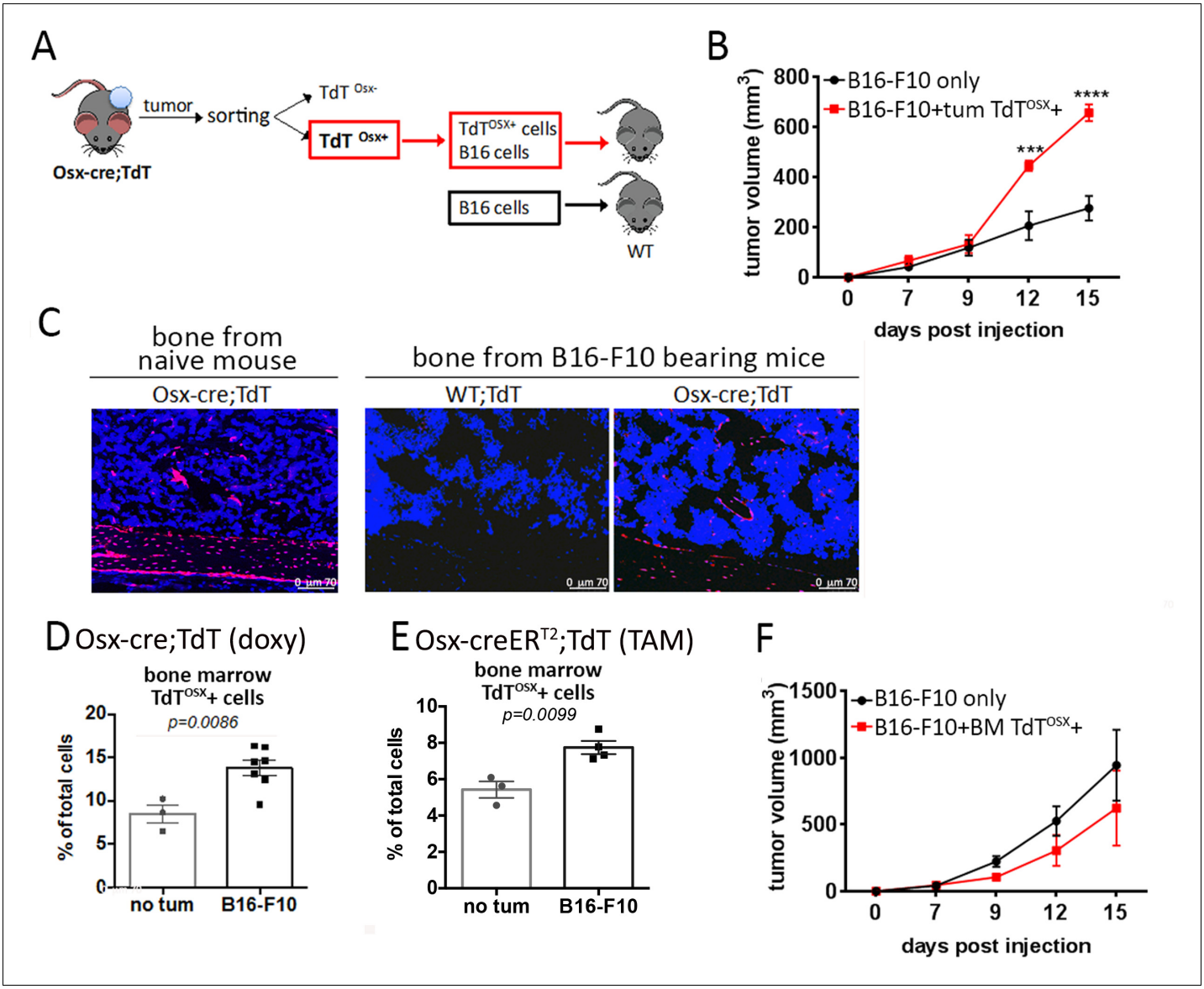

Figure 3. Tumor resident but not bone marrow resident TdT^{OSX}+ cells increase tumor growth. (**A**) Model showing isolation of TdT^{OSX}+ cells from B16-F10 primary tumors injected into doxy-fed Osx-cre;TdT mice and re-inoculation of TdT^{OSX}+ cells together with B16-F10 tumor cells into WT recipient mice at the ratio 5:1. Mice injected with B16-F10 alone were used as controls. (**B**) Tumor growth of experimental model described in (**A**) determined by caliper measurement. n = 3/group, experiment repeated twice. Significance was determined by one-way ANOVA with Tukey post-hoc test. (**C**) Fluorescence images of bone sections showing presence of TdT^{OSX}+ within the bone and bone marrow of naïve Osx-cre;TdT, Osx-cre;TdT mice inoculated subcutaneously with B16-F10 tumors or WT;TdT mice used as negative control. Sections were counterstained with DAPI (blue), magnification 200X. (**D–E**) Quantification of TdT^{OSX}+ cells in the bone marrow of tumor-free and B16-F10 tumor bearing (**D**) Osx-cre;TdT mice (doxy-fed) and (**E**) Osx-creER^{T2};TdT (TAM-treated) determined by FACS. Experiment repeated twice. Significance was determined by student t-test statistical analysis. (**F**) Tumor growth of WT mice inoculated with bone marrow-derived TdT^{OSX}+ cells from B16-F10 bearing doxy-fed Osx-cre;TdT mice together with B16-F10 tumor cells (ratio 5:1). Mice injected with B16-F10 alone were used as controls. n = 3/group. Significance was determined by two-way ANOVA followed by Tukey post-hoc test. ***p<0.001, ****p<0.0001.

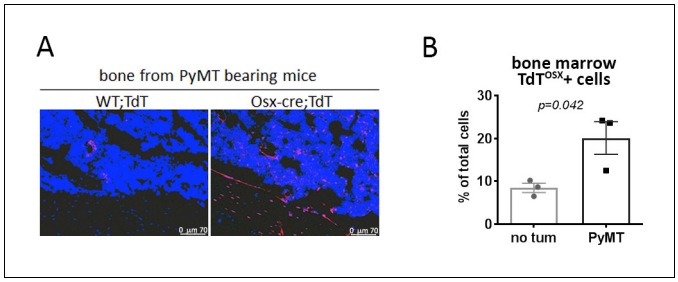

Figure 3—figure supplement 1. TdT^{OSX}+ cells increase in the bone marrow of PyMT tumor bearing mice. (**A**) Fluorescence images of WT;TdT and Osx-cre;TdT mice inoculated with PyMT tumors in the MFP. Slides for fluorescence images were counterstained with DAPI (blue), magnification 200X. (**B**) Quantification of TdT^{OSX}+ cells in the bone marrow of tumor-free and PyMT bearing mice. Experiment repeated twice. p value represents Student t-test statistical analysis.

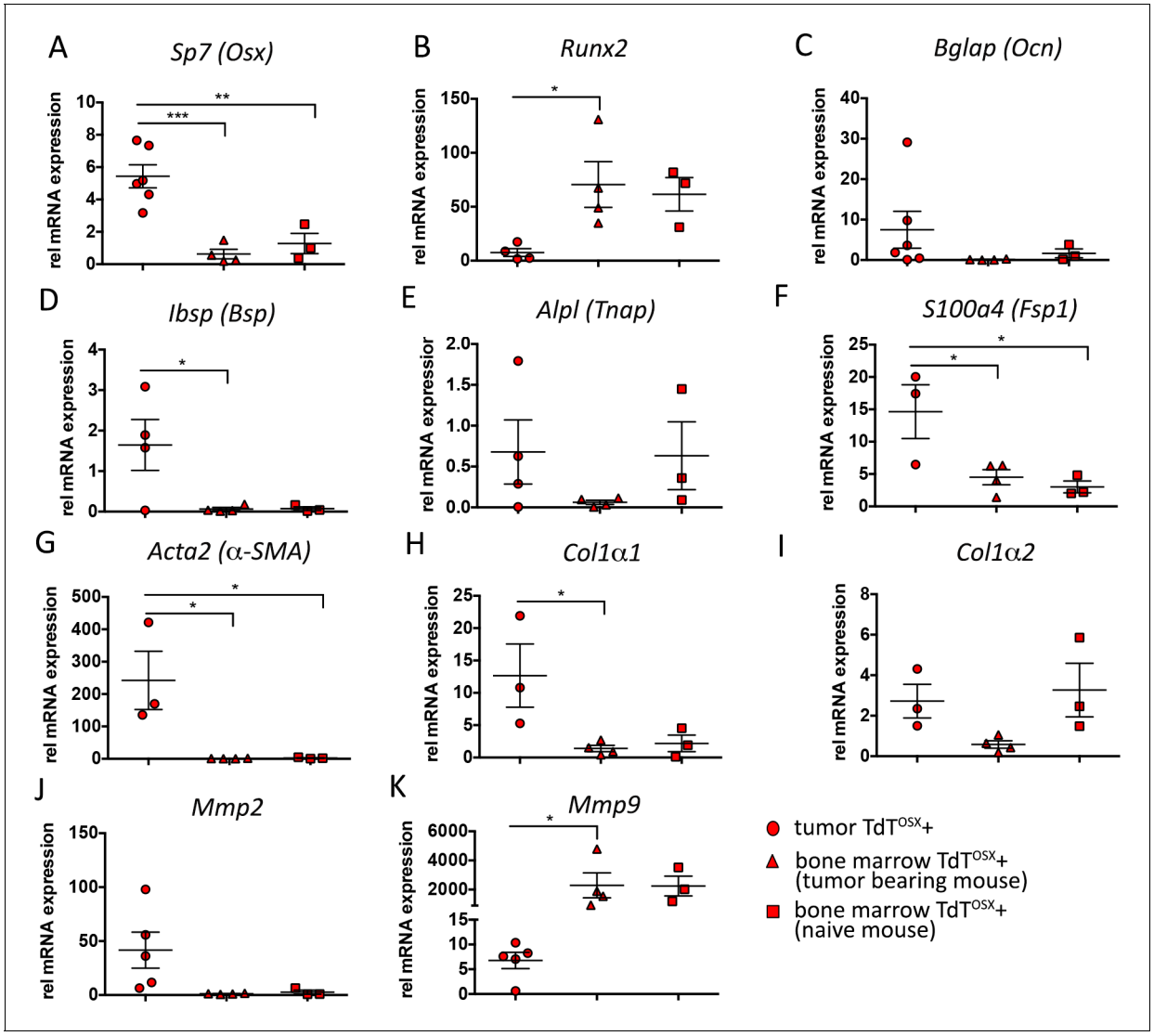

Figure 3—figure supplement 2. Differential expression of mesenchymal markers in TdT^{OSX}+ cells isolated from tumor site or bone marrow. (**A–K**) Quantitative Real-Time PCR for (**A**) *Sp7 (Osterix)*, (**B**) *Runx2*, (**C**) *Bglap (Osteocalcin)*, (**D**) *Ibsp (Bone sialoprotein)*, (**E**) *Alpl (Tnap, Tissue non-specific alkaline phosphatase)*, (**F**) *S100a4 (Fsp1)*, (**G**) *Acta2 (α-SMA)*, (**H**) *Collagen 1a1*, (**I**) *Collagen 1a2*, (**J**) *Mmp2 (Metalloproteinase2)* and (**K**) *Mmp9 (Metalloproteinase9)* genes in TdT^{OSX}+ isolated from the B16-F10 melanoma primary tumors, bone marrow of B16-F10 bearing mice and bone marrow of naïve tumor-free mice.

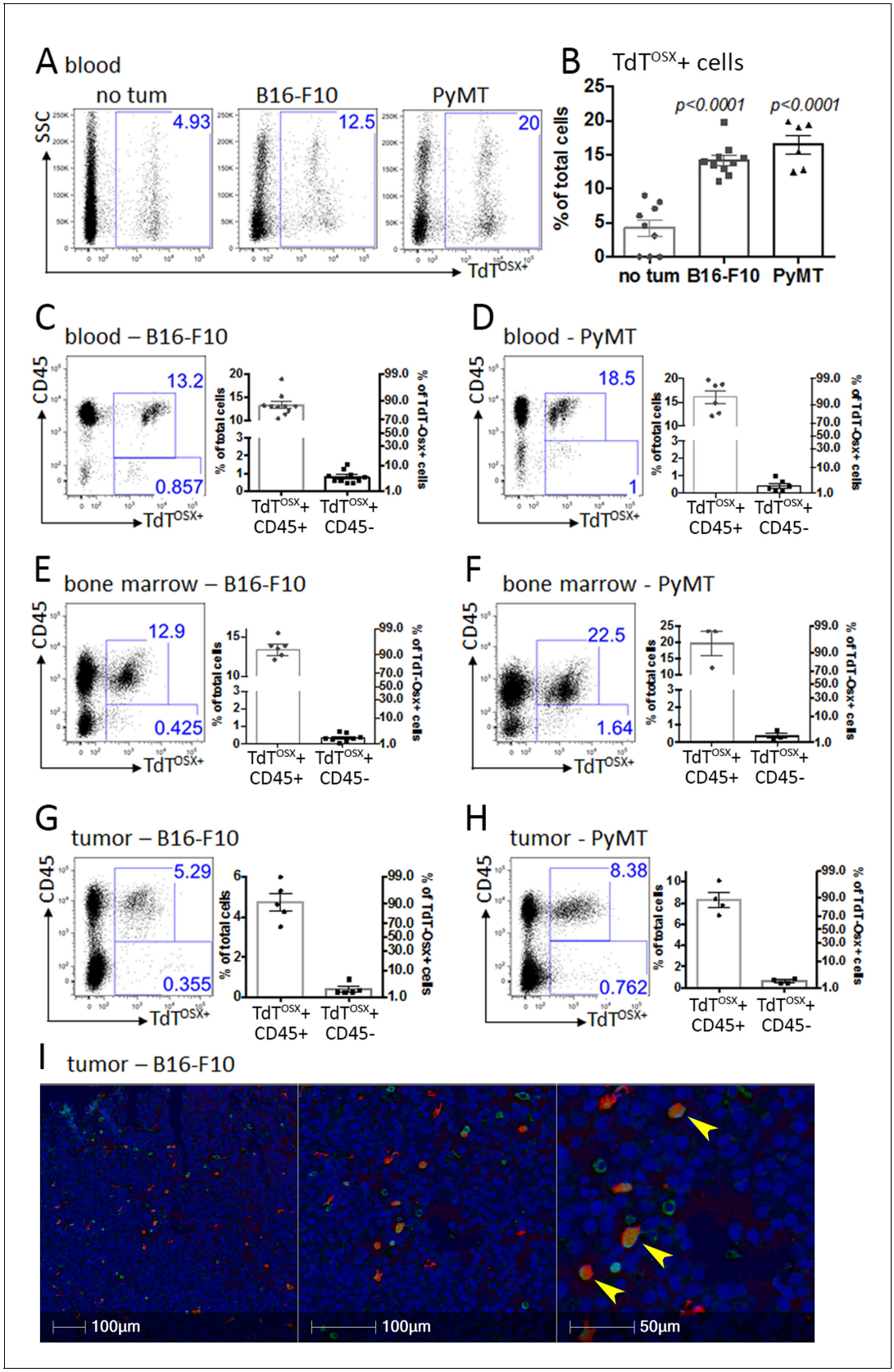

Figure 4. TdT^{OSX}+ cells express the immune surface marker CD45. (**A–B**) Representative FACS dot plots and quantification of TdT^{OSX}+ cells in the peripheral blood of tumor-free and B16-F10 or PyMT tumor bearing mice. Significance was determined by student t-test statistical analysis for each

Figure 4 continued on next page

Figure 4 continued

tumor model relative to no tumor controls. (**C–D**) Representative FACS dot plots and quantification of TdT^{OSX}+;CD45+ and TdT^{OSX}+;CD45- populations in the blood of doxy-fed Osx-cre;TdT mice injected with B16-F10 or PyMT cells. (**E–H**) Representative FACS dot plots and quantification of TdT^{OSX}+;CD45+ and TdT^{OSX}+;CD45- populations in the bone marrow (**E–F**) or tumor site (**G–H**) of doxy-fed Osx-cre;TdT mice injected with B16-F10 or PyMT cells, respectively. Experiments were repeated at least twice. (**I**) Immunohistochemistry staining of paraffin-embedded B16-F10 tumors inoculated into Osx-cre;TdT reporter mice, pseudo colored with red representing TdT^{OSX}+ cells (RFP stained), green representing CD45+ cells (DAB stained) and blue representing nuclei (hematoxylin), magnification 200X.

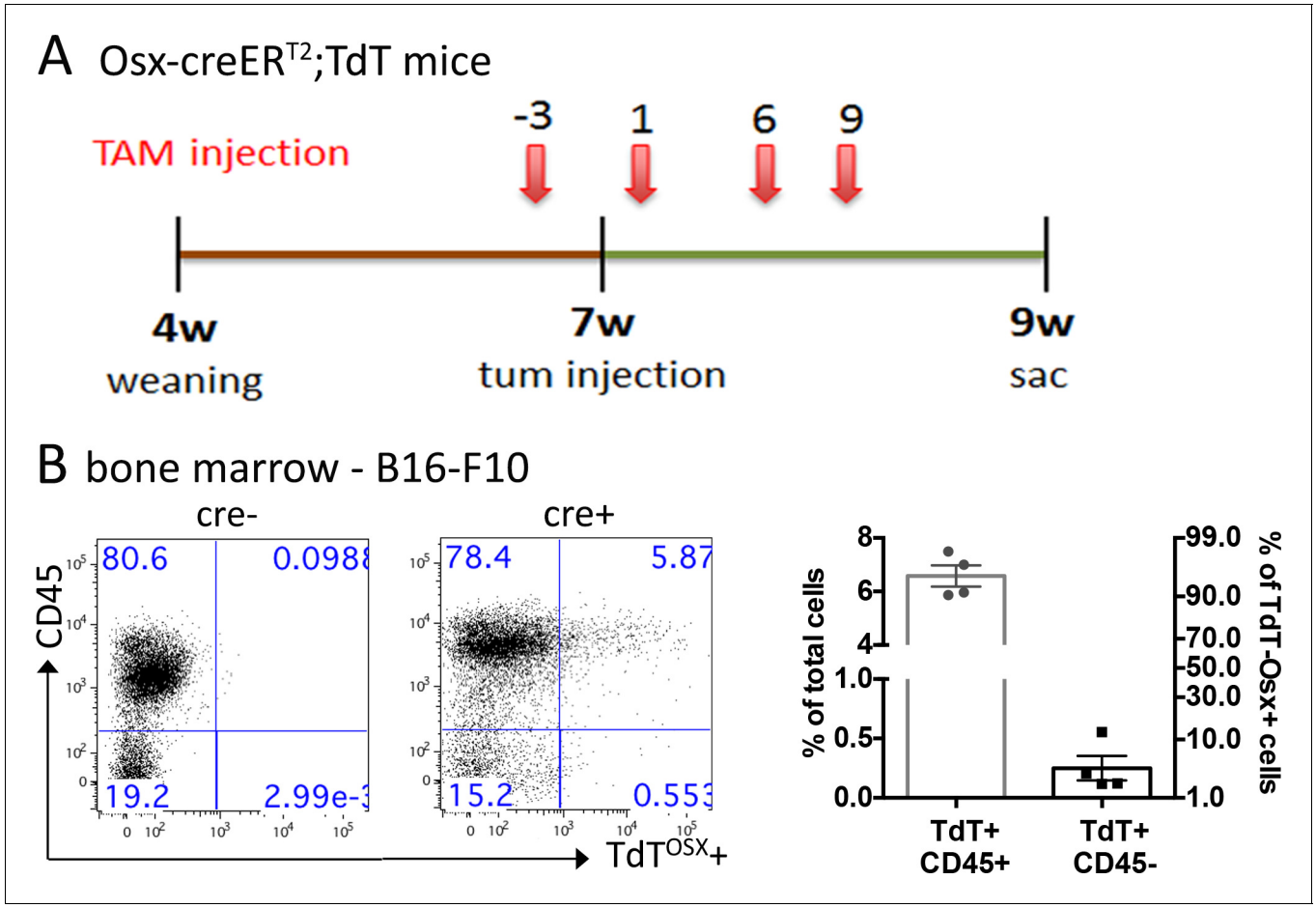

Figure 4—figure supplement 1. Presence of TdT^{OSX}+ cells in bone marrow (BM) of TAM-pulsed Osx-creER^{T2};TdT reporter mice. (**A**) Schematic representation of TAM administration and tumor injection in Osx-creER^{T2};TdT mice. (**B**) Representative image of flow cytometry dot plots and quantification of TdT^{OSX}+;CD45+ and TdT^{OSX}+;CD45- populations in the bone marrow of B16-F10 bearing mice. A cre negative mouse was used as control to set gates. Experiment was repeated three times.

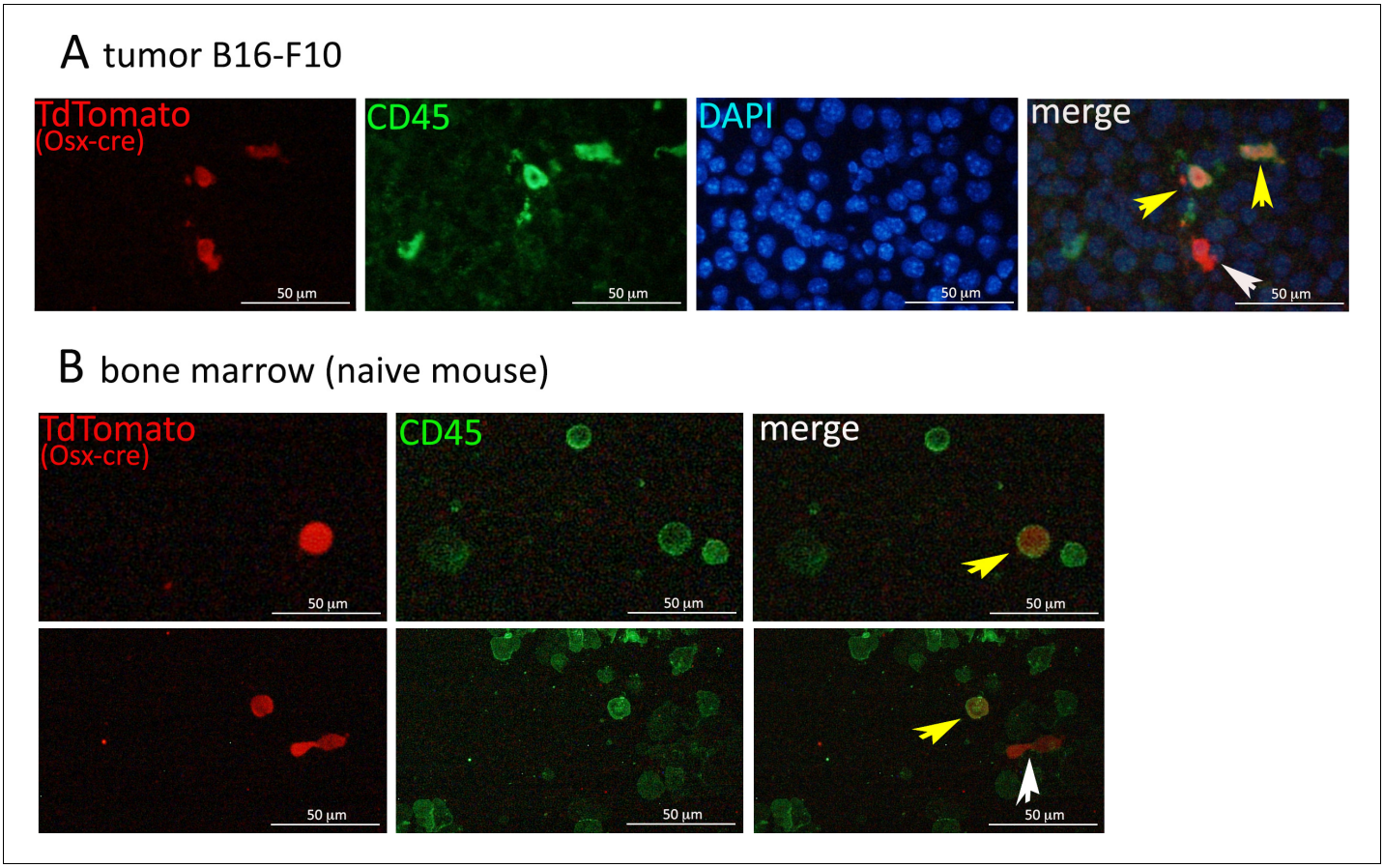

Figure 4—figure supplement 2. Co-expression of Osx-driven TdTomato and the immune marker CD45. (**A**) Immunofluorescence on paraffin-embedded B16-F10 tumors isolated from Osx-cre;TdT reporter mice. Staining was done using anti-RFP (red) to detect TdTomato and anti-CD45 (green) to stain immune populations. Slides were counterstained with DAPI (blue), magnification 200X. (**B**) Staining for CD45 on a single cell suspension from bone marrow of Osx-cre;TdT reporter mice, magnification 200X. Yellow arrows point to TdT^{OSX}+ single cells expressing CD45, while the white arrow points to a TdT^{OSX}+ cell negative for CD45.

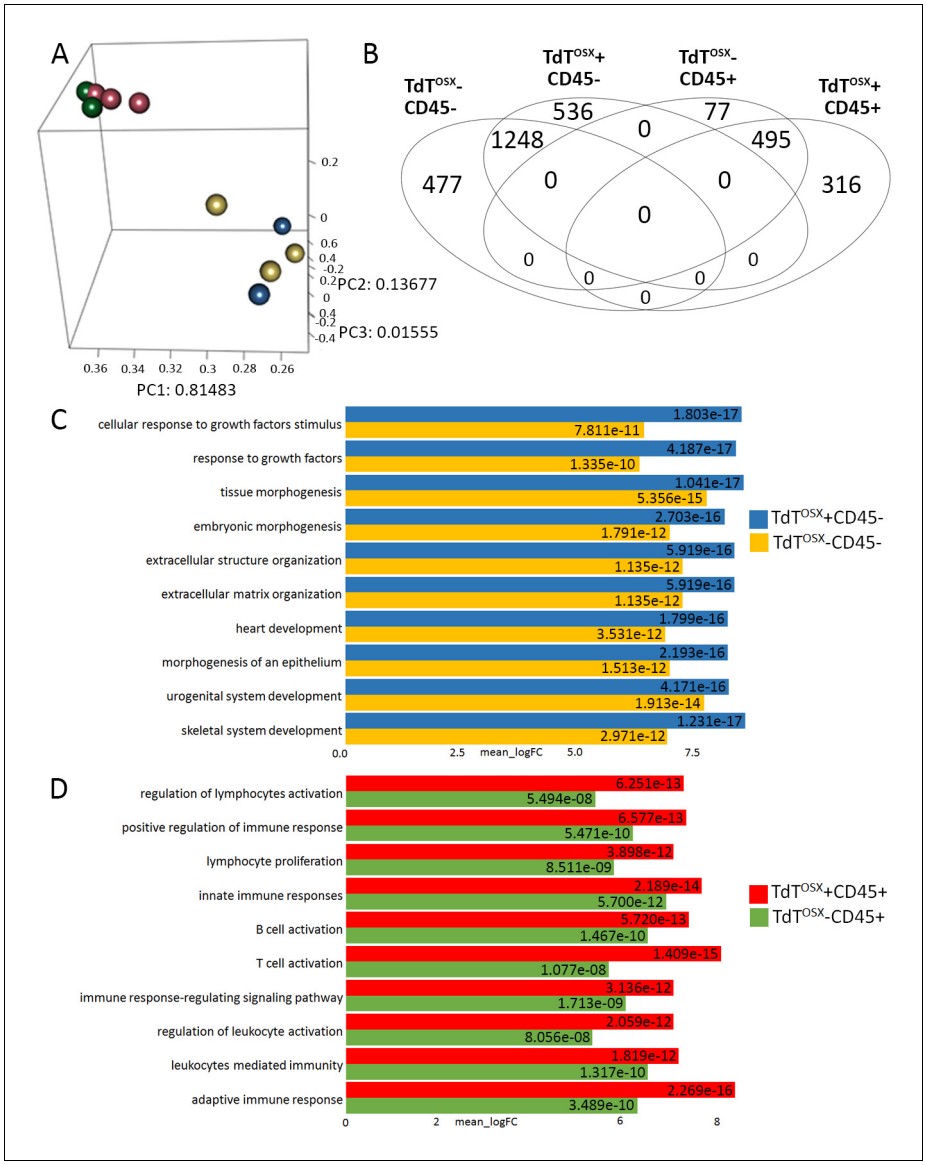

Figure 5. TdT^{OSX}+;CD45- and TdT^{OSX}+;CD45+ are two functionally distinct populations in the tumor microenvironment. (**A**) Multidimensional Principal Component Analysis of RNAseq data obtained from four tumor stroma subsets sorted according to TdT^{OSX} and CD45 expression. (**B**) Venn diagram depicting uniquely and commonly expressed genes among the four groups. (**C–D**) First ten GO pathways obtained from the GO analysis of the log two fold-changes for (**C**) CD45 negative subsets and (**D**) CD45 positive subsets.

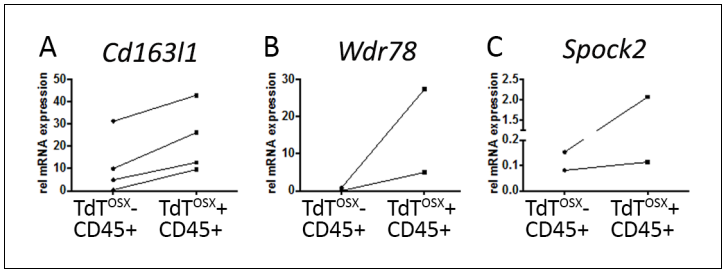

Figure 5—figure supplement 1. Validation of RNAseq data. Real Time PCR performed on TdT^{OSX}+;CD45+ and TdT^{OSX}+;CD45- populations sorted from B16-F10 tumors in doxy-fed mice. Each sample is a pool of two tumors. Data show three genes (**A**) *Cd163l1*, (**B**) *Wdr79* and (**C**) *Spock2* to be upregulated in the TdT^{OSX}+;CD45+ compared to TdT^{OSX}-;CD45+ cells.

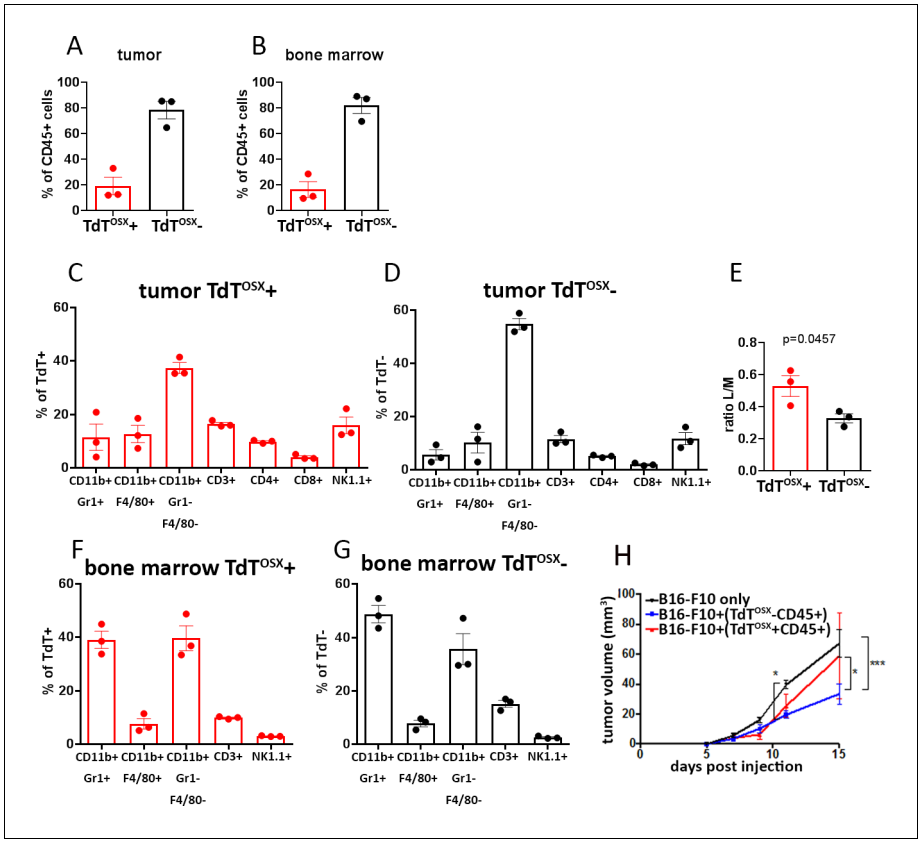

Figure 6. Subsets of myeloid and lymphoid cells in the tumor microenvironment and the bone marrow are derived from TdT^{OSX}+ cells. (**A–B**) Quantification of FACS analysis showing the percentage of TdT^{OSX}+;CD45+ and TdT^{OSX}-;CD45+ populations in the tumor and bone marrow of Osx-cre;TdT mice injected subcutaneously with B16-F10 tumor cells. Data showed as % of total CD45+ cells. (**C–D**) Quantification of FACS analysis showing the percentage of tumor infiltrating myeloid and lymphoid populations within the TdT^{OSX}+;CD45+ or TdT^{OSX}-;CD45+ subsets, each considered as 100%. (**E**) Lymphoid over myeloid ratio within the tumor infiltrating TdT^{OSX}+;CD45+ or the TdT^{OSX}-;CD45+ subsets. Statistical analysis was performed by student t-test. (**F–G**) Quantification of FACS analysis showing the percentage of the bone marrow resident myeloid and lymphoid populations within the TdT^{OSX}+;CD45+ or TdT^{OSX}-;CD45+ subsets, each considered as 100%. n = 3/group. (**H**) Tumor growth in mice injected with B16-F10 tumor cells alone or together with tumor-derived TdT^{OSX}+;CD45+ or TdT^{OSX}-;CD45+ cells at the ratio 1:5. n = 3–6/group.

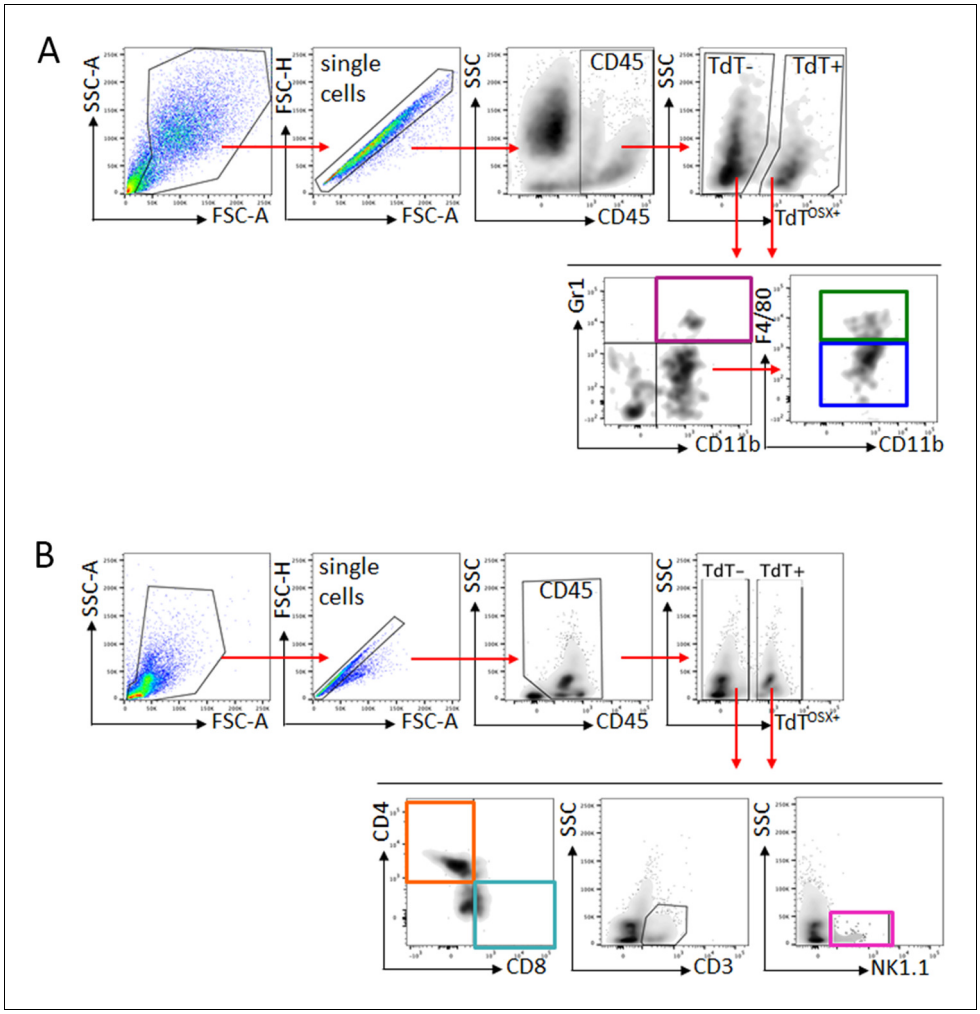

Figure 6—figure supplement 1. Gate strategy for immune staining of tumor and bone marrow. (**A**) Representative gate strategy analysis of total tumor mass stained for CD45, myeloid immune markers CD11b, F4/80 and Gr1. Analysis performed in both TdT^{OSX}+ and TdT^{OSX}- populations. Identical analysis was performed on BM samples. (**B**) Representative gate strategy analysis of BM stained for lymphoid immune markers CD3, CD8, CD4 and NK1.1. Analysis performed in both TdT^{OSX}+ and TdT^{OSX}- populations. Identical analysis was performed on tumor samples. Fluorescence minus one (FMO) controls were used to set the gates. WT;TdT mice were used to set the gate for TdT+ cells.

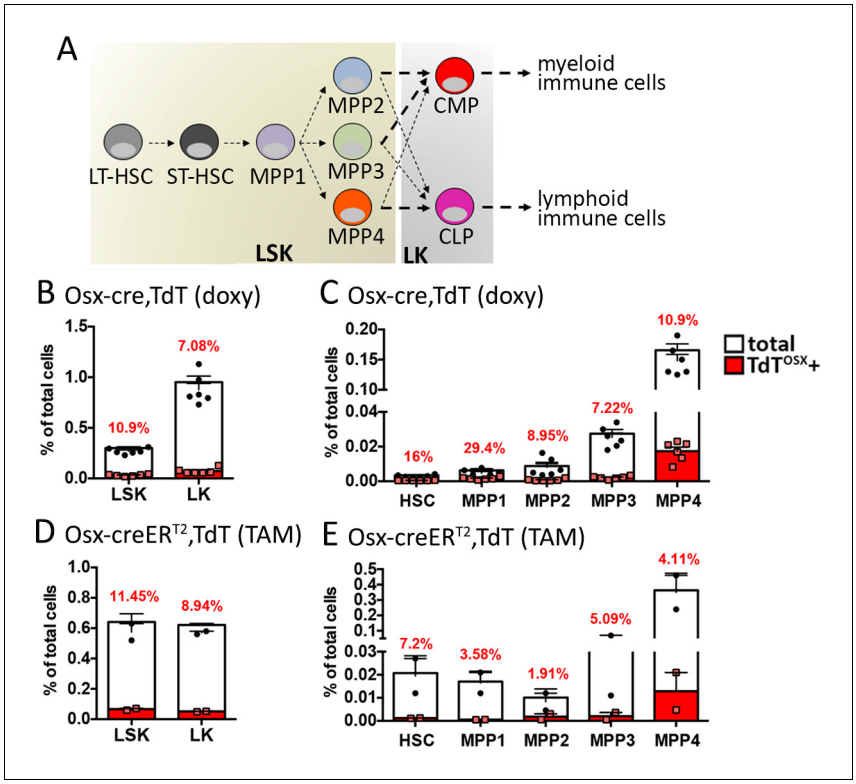

Figure 7. TdT^{OSX}+;CD45+ cells derive from TdT^{OSX}+ HSCs. (**A**) Schematic of hematopoietic differentiation. (**B–E**) Flow cytometry quantification of TdT^{OSX}+ cells in the bone marrow of (**B–C**) doxy-fed Osx-cre;TdT mice and (**D–E**) TAM-treated Osx-creER^{T2};TdT mice injected subcutaneously at 7 weeks of age with B16-F10 tumors. In (**B and D**) LSK and LK subsets are shown, while in (**C and E**) the LSK population is further divided into HSCs and MPP1-4 subsets. Red numbers represent the average of TdT^{OSX}+ cells in each specific subset. n = 2–6/group.

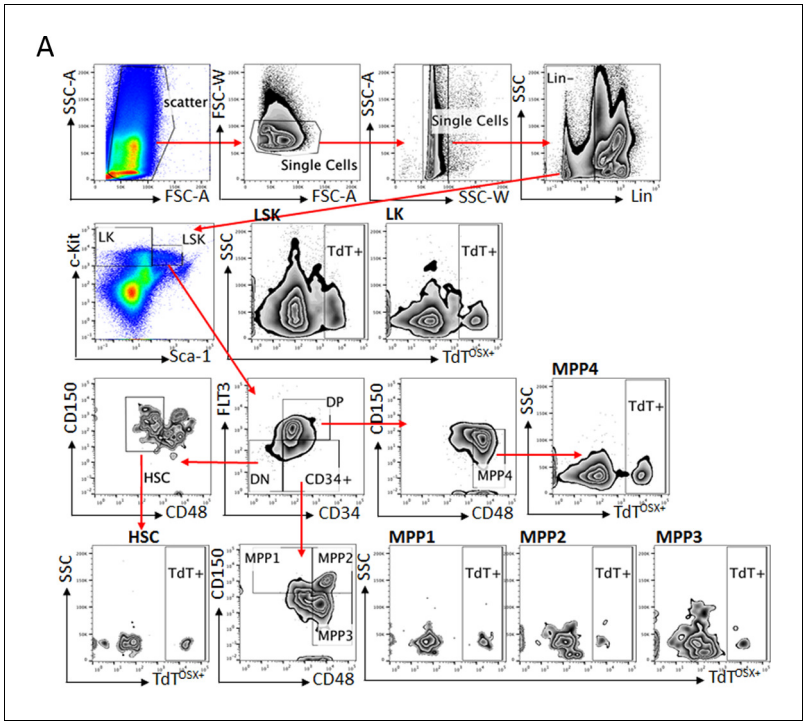

Figure 7—figure supplement 1. Gate strategy for HSC immunostaining of bone marrow. (**A**) Representative gate strategy analysis of bone marrow stained for HSC subsets. TdT^{OSX}+ cells were quantified in each subset. Fluorescence minus one (FMO) controls were used to set the gates. WT;TdT mice were used to set the gate for TdT+ cells.

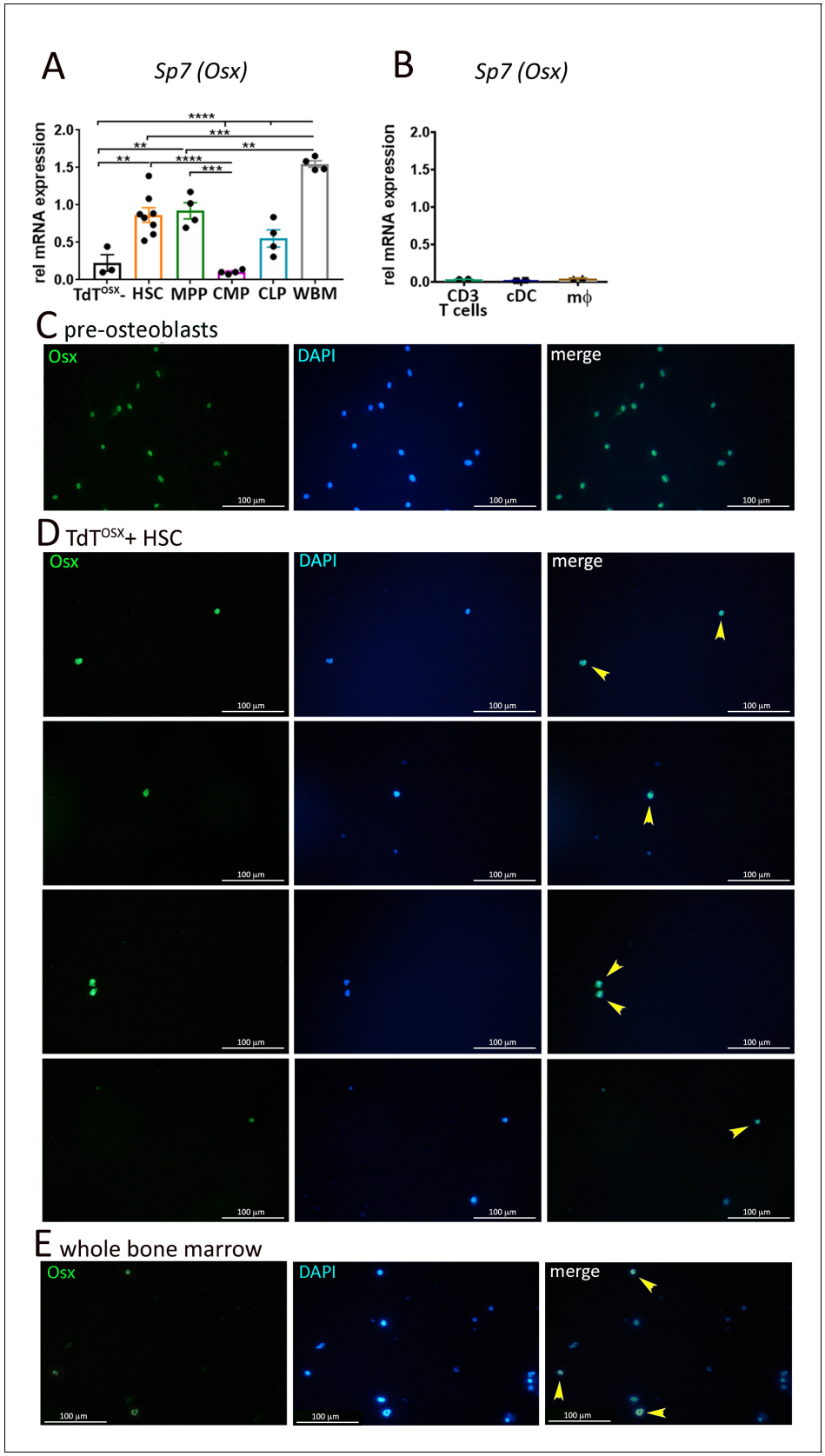

Figure 8. *Sp7* transcripts and Osx protein are expressed in a subset of HSCs isolated from bone marrow of naïve mice. (**A**) Real Time PCR analysis comparing sorted hematopoietic stem cells (HSC), multipotent progenitors (MPP), common myeloid progenitors (CMP), common lymphoid progenitors

Figure 8 continued on next page

Figure 8 continued

(CLP) and whole bone marrow (WBM) from 7 to 9 week old mice. FACS sorted TdT^{OSX}- cells from the tumor of Osx-cre;TdT mice were used as negative control (n = 3–8/group). Statistical analysis was determined by two-way ANOVA followed by Tukey post-hoc test. *p<0.05, **p<0.01, ***p<0.001, ****p<0.0001. (**B**) Real Time PCR analysis of isolated mature CD3+ T cells, conventional dendritic cells (cDC) and bone marrow-derived macrophages (mφ) from WT naïve mice. (**C–E**) Immunofluorescence for Osx in (**C**) primary osteoblasts differentiated from BMSC cultured for 4 days in osteogenic media, (**D**) TdT^{OSX}+ HSCs sorted from Osx-cre;TdT reporter mice and (**E**) whole bone marrow cells from WT mice. DAPI is used for nuclear staining. Magnification 200X.